IEEE Open Journal of the Communications Society

Received 29 September 2022; revised 20 October 2022; accepted 25 October 2022. Date of publication 28 October 2022; date of current version 8 November 2022.

Digital Object Identifier 10.1109/OJCOMS.2022.3217778

A Bandwidth Efficient Hybrid Multilevel Pulse Width Modulation for Visible Light Communication System: Experimental and Theoretical Evaluation

MOHAMMAD ABRAR SHAKIL SEJAN [1] (Member, IEEE), RAMAVATH PRASAD NAIK [2], BOON GIIN LEE [3] (Senior Member, IEEE), AND WAN-YOUNG CHUNG [1,2] (Senior Member, IEEE)

[1]Department of Electronic Engineering, Pukyong National University, Busan 48513, Republic of Korea

[2]Research Institute of Artificial Intelligence Convergence, Pukyong National University, Busan 48513, Republic of Korea

[3]Nottingham Ningbo China Beacons of Excellence Research and Innovation Institute, School of Computer Science, University of Nottingham Ningbo China, Ningbo 315100, China

CORRESPONDING AUTHOR: W.-Y. CHUNG (e-mail: wychung@pknu.ac.kr)

This work was supported by the National Research Foundation (NRF) of Korea Grant funded by the Korea Government under Grant 2020R1A4A1019463.

ABSTRACT Visible light communication (VLC) is considered a new technology for interconnecting devices in 5G and beyond. VLC can provide additional bandwidth for communicating devices which can help to reduce the radio frequency bandwidth congestion. In this work, we aim to maximize the bandwidth usages for VLC. The proposed modulation technique can impose more bits due to the combined utilization of both pulse height and width changes. Moreover, we subdivide the single bit duration to impose more bits for data transmission. The proposed modulation is capable of transmitting more bits by utilizing fewer optical pulses than other traditional modulation techniques such as multilevel modulation, on-off keying, pulse width modulation, pulse position modulation, pulse amplitude modulation, and multiple pulse position modulation. We have evaluated the theoretical bit error rate (BER) expression in terms of average signal to noise ratio and compared the experimental BER performance for the proposed system. The experimental results demonstrate that the proposed modulation technique can achieve a communication distance of 3 m in an indoor environment.

INDEX TERMS Modulation, visible light communication, optical communication system, indoor VLC.

I. INTRODUCTION

VISIBLE light communication (VLC) a promising technology for indoor wireless connectivity because of its large unregulated bandwidth, security, electromagnetic interference-free communication, and high data-rate [1]. VLC can be easily integrated with the existing infrastructure to serve the dual purpose of illumination and communication at the same time [2], [3]. The visible light spectrum ranges from 380 *nm* to 750 *nm*, corresponding to a frequency spectrum in the range of 430 *THz* to 790 *THz* [4]. This large bandwidth is available for use without a license. Consequently, RF spectrum congestion can be reduced by interconnecting Internet of Things (IoT) devices using this bandwidth [5]. In VLC, the main component used for transmission is light emitting diode (LED), which is available at low price, has a long-life cycle, and consumes low energy [6]. At the receiver end, a photo-diode or a complementary metal-oxide-semiconductor (CMOS) camera can be used as the receiving device. The light intensity is modulated to transmit the data, which are directly detected by the photo-detector or CMOS camera.

Various modulation techniques are available for VLC data transmission. Single carrier modulation, multi-carrier modulation, and color-domain modulation are included in these techniques. Single carrier modulations (SCM) are straightforward and easy to implement. It includes on-off keying (OOK), variable pulse position modulation (VPPM), pulse position modulation (PPM), pulse width modulation (PWM) and pulse amplitude modulation (PAM) [7]. The multi-carrier modulation technique achieves high spectral efficiency, but exhibits computational complexity, such as orthogonal frequency division multiplexing.

In most cases, OOK is employed in VLC because it is straightforward and easy to implement. A signal pulse is represented by the binary bit 1, and no pulse is represented by 0. PWM is useful in dimming control, and the pulse duration is varied to represent the data bits. In PPM, the position of the pulses is varied to represent the bit patterns. Multiple pulse position modulation (MPPM) is an extension of PPM, where multiple pulse position combinations represent different bits. PAM can transmit data by varying the amplitude of signal. Each modulation technique has its advantages and disadvantages in terms of data-rate and dimming control. In addition, these techniques do not allow high data-rates due to bandwidth wastage by the compensation time interval [8]. These limitations provide the motivation to investigate a more efficient bandwidth utilization solution than that achieved by the existing modulation techniques.

In this work, a hybrid modulation technique capable of transmitting more bits than the existing techniques is proposed. PAM or multilevel modulation transmits bit information by changing the pulse amplitude or height as a power of 2. In PWM information bits are transmitted by changing the pulse width duration. A combined approach multilevel pulse width modulation (MPWM) can increase the data-rate because both pulse height and width changes are considered simultaneously to send data bits. In the MPWM scheme we sub-divide the single bit duration into 4 segments. Four levels of multilevel modulation and four different PWM widths can generate 16 unique combinations for transmitting data. For synchronization purpose we add an extra segment to mark ending of a 4-bit pulse duration. As a result, bandwidth wastage due to time interval compensation can be reduced. The proposed modulation scheme is experimentally tested using an array of 3×3 LEDs. A communication distance of 3 m can be achieved with an acceptable error rate. The contribution of this study can be summarized as follows:

- A new modulation scheme is proposed to reduce the time compensation interval for SCM by utilizing the pulse width and height at the same time. 16 different combinations of the signal were generated by subdividing the single bit duration, and each can convey 4 bits.
- A comparative analysis was provided to show the impact of the proposed modulation with the traditional techniques. The combined approach can transmit more data bits in fewer optical pulses.
- Proposed hybrid multilevel pulse width modulation implemented for the indoor VLC link experimentally.
- Evaluated the theoretical bit error rate (BER) expression of the proposed system and compared the theoretical BER performance with the experimental BER performance in terms of average signal to noise ratio (SNR).

The rest of this paper is organized as follows. Previous related research work is presented in Section II. Details of the proposed modulation technique and the related algorithms are presented in Section III. The experiment setup is described in Section IV. The proposed VLC link evaluated theoretically in Section V. Obtained results and corresponding discussions are described in Section VI. Finally, the paper is concluded in Section VII.

II. RELATED WORKS

IEEE 802.15.7 describes three modulation techniques, namely, OOK, VPPM, and color shift keying (CSK) [9]. Other types of modulations suitable for VLC were discussed in [10] and suggested for further reading. In this work, we focus on the state-of-the-art multilevel and PWM.

Rachim et al. proposed a four-level modulation technique to achieve a communication distance of 2 m in [11]. The system was implemented using a mobile phone camera for data reception to obtain indoor position using VLC. A modified Hadamard code-based multilevel modulation method was proposed for the indoor positioning system in [12]. A two-level OOK signal for light fidelity (LiFi) communication was presented to overcome the flickering problem [13]. In [14], the authors proposed a gamma function based pre- and post-compensation technique to overcome the nonlinearity problem in optical camera communication (OCC) and improve the performance of the multilevel modulation system. Authors in [15], proposed an enhanced multi-level multi-pulse modulation which provides uniform illumination with dimming control capability for MIMO VLC.

PWM is also widely used modulation technique in VLC. The pulse duration is varied to represent the signal's data value. In [16], PPM and PWM were combined to achieve data transmission transmit data in a 20 cm distance. Authors in [17], experimentally demonstrated a different PWM for the bit-pattern transmission. PWM is used to produce different levels of data transmitted to a mobile phone in [18]. In [19], a variable pulse amplitude and position modulation scheme was proposed for a dimmable VLC system. Ntogari et al. [20] proposed PWM dimming with discrete multitone signals to transmit data over a VLC channel. In [21], the authors proposed a combination of PPM and PWM to control the dimming level. The width of a PWM pulse was made proportional to the dimming level of illumination, and PPM modulated data signals for transmission.

Previous studies in the literature have also proposed hybrid modulation for VLC. The study in [22], proposed multilevel multiple pulse position modulation for joint brightness and data-rate control. Three parameters were considered slot number, level of brightness and accumulated weight for creating symbol. Brightness controlling was achieved by fixing the slot number and brightness level which changing the weight. Another hybrid modulation technique was proposed in [23], that combines three approaches PWM, PPM and discrete pulse amplitude modulation (DPAM) for CMOS camera. In each signal period both width and phase of the signal convey data bits. Authors employed DPAM for keeping the LED luminous flux constant in each signal period. In [24], the authors proposed a generalized spatial

modulation with multi-pulse amplitude and position modulation. Multiple pulse position modulation and pulse amplitude first used to make the transmission signal and then specific LEDs are chosen to transmit data. Two level of amplitude were employed in case of pulse amplitude. In [25], authors proposed a convolutional encoder of trellis coded modulation in M-ary phase shift keying-color shift keying (MPSK-CSK) in VLC. PSK complex signals are converted to HSV color space and RGB-LED is used to transmit data. The transmitted signal is received by color photodetector and Viterbi algorithm to decode the data. Another hybrid modulation approach was proposed in [26], with laser diode based M-ary differential phase-shift keying and a two level multipulse pulse-position modulation for improved spectral efficiency. Pulse position modulation with Gaussian minimum shift keying was proposed in [27], to minimize the inter symbol interference for cellular backhaul channel. In [28], the authors proposed a mixed interleave multi-pulse position modulation where information bits are sent using a header and data frame. The proposed modulation does not use continuous pulse in the data section. This helps to reduce the cases to consider as a single pulse and easily distinguish multi-pulse.

In MPWM, we propose to combine PAM and PWM to increase the number of bits in transmission. We choose to divide the single bit duration into 4 segments and each segment can transmit 4 bits. Among the previous studies [23] and [24] are closely related to our study. The study in [23], used PWM and PPM in one signal period to represent binary data for 8 constellation points 3 bits can be transmitted. In addition, DPAM is used for dimming control with pulse width fixed. In the case of [24], MPPM and MPAM are combined to make MPAPM for data transmission with GSM for MIMO communication. In our approach, we combined PWM and PAM to create a data signal which can transmit 4- bits, and pulse width change is dynamic. Pulse width can vary depending upon the input binary data and can be successfully demodulated in the receiver end for SISO communication. Thus, it can be possible to increase the data-rate in a single pulse duration by reducing time interval compensation. At the end of each 4-bit transmission, one extra pulse is added for synchronization. It is necessary to correctly demodulate the data when we change the pulse width. Both axis changes are utilized to transmit data as an impact of this more information bits can be transmitted over the channel. Signal demodulation is performed by first determining the signal level and then the signal duration. The signal level is determined by the first two bits, and the pulse duration is determined by the next two bits.

III. PROPOSED MODULATION AND DEMODULATION

Four different amplitude levels, which can be represented by four two-bits combinations, are presented in Fig. 1(a). The lowest signal amplitude is l_1, which is increased by l_2, l_3 and l_4 times to represent different amplitude levels. Four different pulse durations τ_1, τ_2, τ_3 and τ_4 are shown in Fig. 1(b). Here τ_4 represents a full duration in which OOK modulation can transmit one bit. These two approaches are combined to generate 4×4 combinations, where each combination represents 4 bits. Figure 2 represents the 16 different combinations obtained when combining the two approaches to produce a hybrid MPWM.

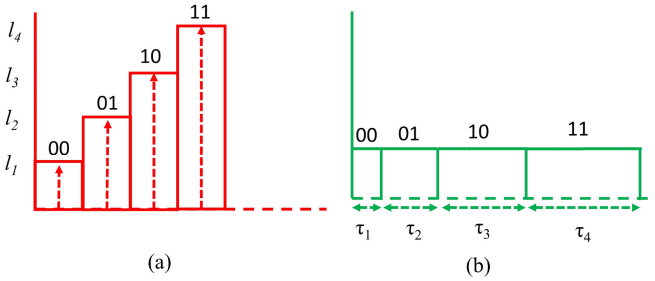

FIGURE 1. (a) Four different amplitude level corresponds to four different distinguishable bit patterns; (b) The pulse width is varied to represent four different states of four distinguishable bit patterns.

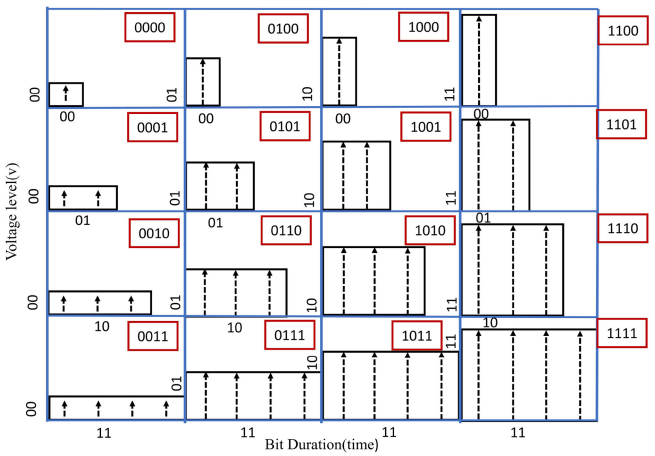

FIGURE 2. By combining multilevel and pulse width modulation 16 different unique signal combinations can achieved, and each signal segment can carry 4 bits; the horizontal axis represents bit duration and vertical axis represents voltage level.

Figure 2 represents level l_1, which corresponds to the first two bits (00). Then, the next two bits are considered. The pulse is varied, according to the second pair of the bits. Each row in the first column represents the pulse-width variation, which corresponds to a four-digit combination. The second column represents the 01 level, which is two times higher than the previous level, i.e., l_2. Each second-column row represents the pulse-width variation. The third column represents the l_3 level for the 10 bit pattern, and the rows represent the pulse width of each second-pair digit. Finally, the fourth column represents level the l_4 level for the bit pattern 11. Each row in the fourth column represents the second pair of variable width bits. The first row has duration τ_1, which represents the 00 bit pattern, and the second row represents width duration τ_2, which represents 01. The third and fourth row has duration τ_3 and τ_4, which represent bits 10 and 11, respectively. To demodulate the signals we need to insert extra pulse to indicate the end of a 4 bit segment. If any

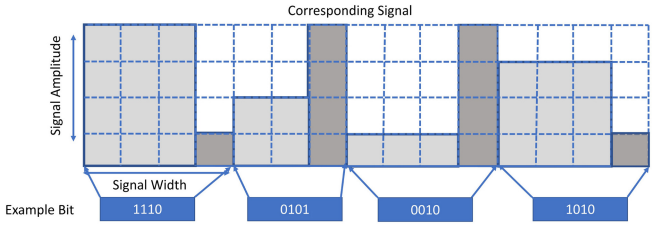

FIGURE 3. An example of the proposed modulation technique for 16 bits; each signal segment represents 4 bits with an ending section for demodulation purpose; the first pair of bits represent the signal level, and second pair of bits represents the signal width.

segment amplitude level ends on l_1 or l_2, then we add an l_4 pulse as ending mark. Again, if any segment ends at l_3 or l_4, then we add an l_1 pulse as ending mark. An example of data signal 1110010100101010 is given in Fig. 3. In best case scenario, when the width is τ_1 the MPWM uses half of single bit duration to transmit 4 bits. And in worst case, when the width is $5 \times \tau_1$ the proposed modulation uses 1.25 times of a single bit duration to transmit 4 bits.

We can represent the modulation by following equation

$$S_{liwi} = \begin{bmatrix} S_{l1w1} & S_{l1w2} & S_{l1w3} & S_{l1w4} \\ S_{l2w1} & S_{l2w2} & S_{l2w3} & S_{l2w4} \\ S_{l3w1} & S_{l3w2} & S_{l3w3} & S_{l3w4} \\ S_{l4w1} & S_{l4w2} & S_{l4w3} & S_{l4w4} \end{bmatrix} \tag{1}$$

where S_{liwj} represents level i and width j.

The main challenge of the demodulation process is to determine the pulse duration of each of the bit sequences. To make the process trackable we have inserted one extra pulse as a guard pulse. The demodulation process is started by extracting the voltage value which is stored for the next value comparison. After each τ_1 time duration, a new voltage value is extracted to observe the change in the voltage level. The following formula is used to determine the pulse duration

$$Pd = \tau_1 \times c + 1 \tag{2}$$

where c the is the counter and $c \in \{0, 1, 2, 3\}$ and $\tau_1 = 1$. The value of τ will vary depending upon the system. The parameter c is counted until the voltage level does not change. Figure 4 shows the demodulation system of the proposed modulation. Figure 4(a) shows the voltage level l_4 and the width counter $c = 2$, that is $\tau_1 \times 2$ before any voltage change, according to Eq. 2 $Pd = 3$. Thus, the demodulated bits are 1110. Similarly, Fig. 4(b), Fig. 4(c), and Fig. 4(d) show the demodulation of bits 0101, 0010, and 1010 respectively.

IV. EXPERIMENT SETUP

In this section we have presented experimental testbed setup and comparison between the proposed modulation with the available modulation techniques.

A. TESTBED DETAILS

The proposed modulation technique was tested by conducting experiments in indoor environment. A transmitter

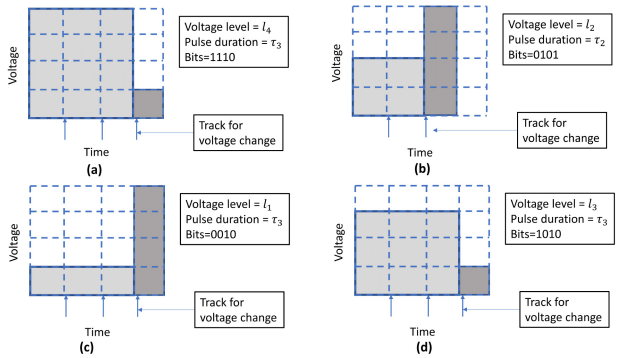

FIGURE 4. Demodulation example of the proposed scheme for four different case scenarios.

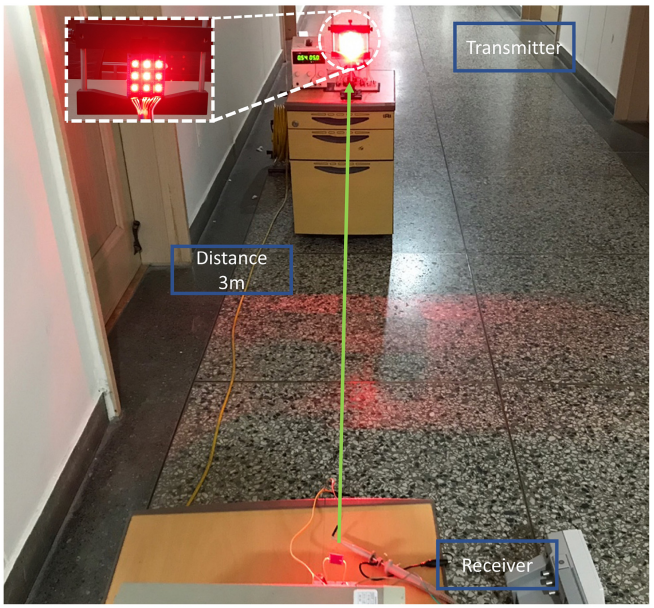

FIGURE 5. Experiment setup for multilevel pulse width modulation applied to a 3 m distance.

consisting of 9 different LEDs (hyper flux red LED of 620-630 nm operating wavelength) was used for data transmission, and a receiver with a single photo-diode (Hamamatsu's S5107 Si photo-diode with 0.45 A/W responsivity at 620 nm wavelength) was used for data reception. The experiment setup is shown in Fig. 5. The transmitter and receiver were placed along a horizontal direction and the light signal directly pointed at the photo-diode using the plano convex lens. This setup provides stable and efficient communication because it avoids reflected light. The transmitter circuit consists of a driver circuit, which regulates the current flow in the LEDs for dimming control. The experimental parameters are listed in Table 1.

1) TRANSMITTER SECTION

Different lighting combinations were used to generate different level signals. The level 1 (bits 00) voltage was produced by turning on 2 LEDs, which generated 250 lux at a 3 m distance. The level 2 (bits 01) voltage was produced by turning

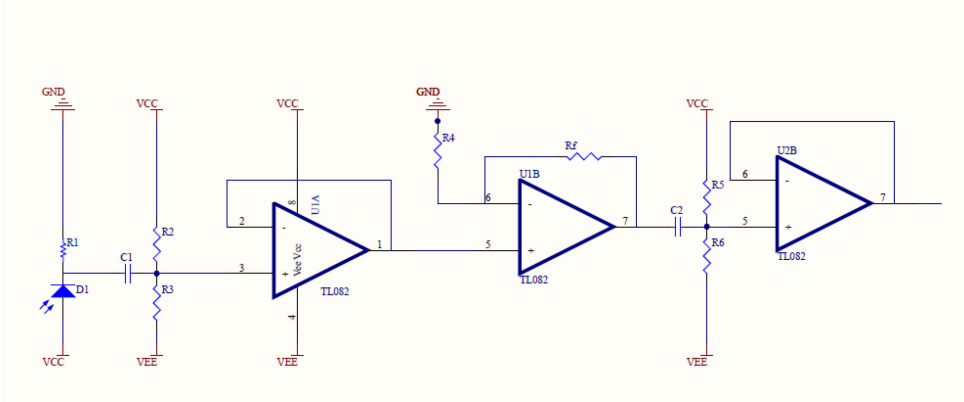

FIGURE 6. The schematic diagram of the received circuit is used to demodulate the proposed modulation technique.

TABLE 1. Experimental parameters.

Parameters	Values
Number of LEDs	9
Number of photo-diodes	1
Experiment area	Indoor & corridor
Distance	1-5m
Lens adapted	Plano-convex
Ambient light	40-200 lux & 350-600 lux
LED viewing angle	0°-100°
receiver photodiode	Hamamatsu S5107
LED	Hyper Flux 5Pie Red
Receiver circuit chip	TL082
Modulation	Proposed MPWM

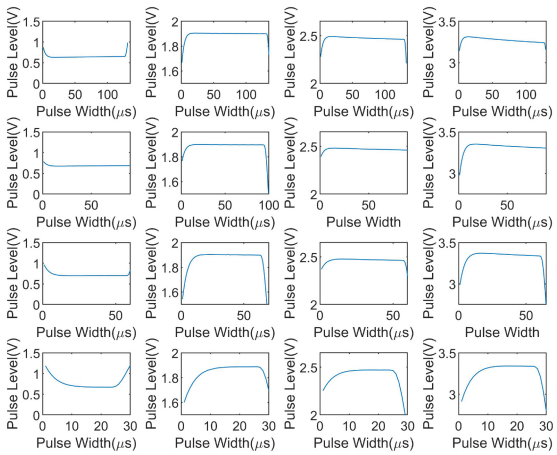

FIGURE 7. Threshold map for distinguishing 16 different signal combinations; the first signal level shown in the first column is in the range 0–1.5 V; the second signal level shown in the second column is in the range 1.6–2 V; the third signal level shown in the third column is in the range 2–2.5 V; the fourth signal level shown in the fourth column is in the range 2.7–3.5 V; The corresponding pulse width is 30, 60, 90, and 120 μs, respectively.

on 4 LEDs, which generated an illumination of 650 lux. The level 3 (bits 10) voltage was produced by turning on 7 LEDs, which generated an illumination of 900 lux. Finally, the level 4 (bits 11) voltage was produced by turning on all 9 LEDs, which generated a maximum illumination of 1150 lux. An Atmega128 microprocessor was used in the transmitter to generate the signal with the corresponding data. Port communication for controlling the LEDs was used to modulate the data. In the driver circuit, four pins were used to illuminate a different number of LEDs each time.

2) RECEIVER SECTION

In the receiving end, a photo-diode circuit was used to receive the optical signal. The ADS8686SEVM-PDK evaluation module was used to capture the data from the optical receiver circuit. The receiver circuit converts the optical signal into a voltage signal, which is amplified to distinguish the different levels. As an initial experiment, we kept the receiver circuit as simple as possible. We have employed two TL082 chips for extracting the voltage change in the received signal. The schematic diagram is shown in Fig. 6. The first TL082 chip is used to amplify with feedback resistance and the second one is normally amplified. In the case of high-speed data transmission, this circuit may not provide optimal performance and need more high-speed operating chips with high-frequency MCUs. Also, the circuit design will be more sophisticated for differentiating voltage levels in long-distance communication. According to the experiment result the circuit will be 2 to 5 times more complex to extract data more than 10 m distance. This issue can be investigated in future research direction. 2^{16} frames were captured at a different distance, and the received frames were stored to calculate bit error rate.

3) THRESHOLD CALCULATION

In the experiment, we capture the data in the optical channel and later we process the data in a PC. First, the threshold was calculated to distinguish the different signal levels. The different threshold levels were defined by the received signal levels as shown in Fig. 7. The threshold levels at a 3-m distance are presented in Fig. 7. The 16 different signal levels shown on Fig. 7 are used to determine the bit values. The first row presents different signal levels for signal duration 4τ, which is 120 μs. The second row presents different signal

levels for signal duration 3τ, which is approximately 90 μs. The third row presents different signal levels for signal duration 2, which is approximately 60 μs, and the fourth row presents different signal levels for signal duration, which is 30 μs. To determine the decision threshold, the corresponding voltage level is also required. The first column in Fig. 7 shows the voltage threshold for 1-level signal values, which are in the range 0.0-1.5 V. Any value out of this range will not be at this level. The second column in Fig. 7 shows voltage threshold for the 2-level signal values, which are in the range of 1.6-2.0 V. Any value out of this range will not be in this level. The third column in Fig. 7 shows the voltage threshold for 3-level signal values, which are in the range of 2.0-2.5 V. Finally, the fourth column in Fig. 7 shows the voltage threshold for 4-level signal values, which are in the range 2.6-3.5 V. The different threshold level values with respect to distance are given in the Appendix. As the received voltage level depends upon the LED illumination the generalized form of the threshold values is hard to identify for arbitrary distances. However, we can bound the different level values by inequality expression. To express the threshold values ranges in a generalized form we can write the following inequalities:

$$l_1 \leq \frac{\max\_a + max\_b}{4}, \tag{3}$$

$$l_2 \leq \frac{\max\_a + max\_b}{3}, \tag{4}$$

$$l_3 \leq \frac{\max\_a + max\_b}{2}, \tag{5}$$

where l_1 is the average voltage value for 1-level, l_2 is the average voltage value for 12-level, l_3 is the average voltage value for 3-level, max $\_a$ is the highest value and max $\_b$ is the lowest value for the range of 4-level voltage value. Also, the value ranges will always satisfy:

$$l_1 < l_2 < l_3 < l_4, \tag{6}$$

where l_4 is the average voltage value for 4-level.

B. MODULATIONS FOR COMPARISON

To demonstrate the advantage of the proposed modulation technique we compared with existing modulation techniques namely OOK, MPPM, PPM, PWM and PAM. In this section we explore the different modulations in brief. The most widely used modulation is OOK, a single light represents a one bit and no light represents 0 bits. The data-rate of OOK depends on the duration of a single bit or one optical pulse. As an illustration purpose the bit sequence 00111001 is considered for all modulation techniques. As shown in Fig. 8(a), the corresponding signal which requires 8 single bit duration or 8 optical pulses. In Fig. 8(b), MPPM modulation depicted, the four combination presented first and the corresponding signal which requires 16 optical pulses. Next in Fig. 8(c) PWM modulation is shown, different pulse duration represents different bits, and the example bits requires 16 optical pulses. In Fig. 8(d) shows PPM, each 3 bits require

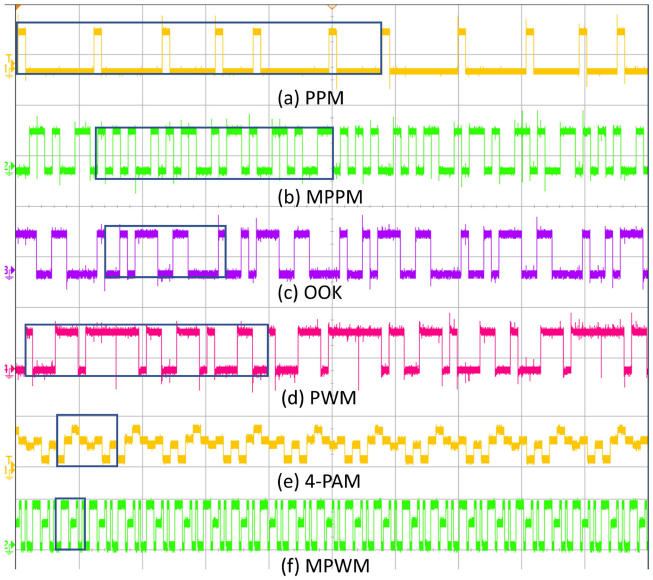

FIGURE 8. The figure shows the frame length comparison of test data 0x2E and 0x61 for different modulation technique; each division represents 1 ms time in x-axis and y-axis in volt.

TABLE 2. Modulation parameters.

Modulation	Encoding method	Data in one Pulse
OOK	1 single bit each pulse	1 bit/pulse
MPPM	2 pulses in 4 slot duration	0.5 bits/pulse
PWM	25%, 50%, 75% and 100% dimming	0.5 bits/pulse
PPM	1 pulse in 8 slot duration	0.375 bits/pulse
PAM	4 amplitude levels	2 bits/pulse
Proposed	4 amplitude levels and 4 widths	4 bits/pulse(avg)

8 optical pulse. Thus, 8 bits require 24 optical pulses, which is caused by time interval compensation. Figure 8(e) shows PAM, which requires only 4 optical pulse to transmit the example bit pattern. And Fig. 8(f) shows the proposed modulation, which requires only 2 optical pulses to transmit the example bit pattern. In Table 2 we listed the modulation parameters and data conveyed in one pulse duration for comparison. The modulations presented in the Fig. 8 we used the same transmitter and received power for proper comparison.

V. THEORETICAL EVALUATION OF THE PROPOSED SYSTEM

The data received by the VLC communication link for the proposed multilevel pulse width modulation is given as [29],

$$Y(t) = hl_i \Pi\left(\frac{t - \frac{\tau_i}{2}}{\tau_i}\right) + n(t) \tag{7}$$

where h is channel fading coefficient or impulse response between LED and Photo-detector, which is function of Lambertian emission pattern and line of sight path between the transmitter-receiver and is given in [15]. In this paper, we have obtain the experimental data (received data) in order to

evaluate the numerical analysis, such as mean and variance. Hence, the set of received data forms a Gaussian distribution with appropriate mean and variance for various levels of intensity as well as duration. l_i and τ_i are amplitude of duration of data, subscript i indicates level of amplitude and duration of the specific data, lies between 1 to 4 for the proposed modulation scheme, $\Pi(\cdot)$ is a rectangular function and n is additive white Gaussian noise with zero mean and σ^2 variance. Source for the noise variance is thermal noise, shot noise and background noise. Signal to noise ratio (SNR) of Eq. (7) is $\gamma = \frac{h^2 l_i^2 \tau_i}{\sigma^2}$ (Signal power $P = \int_{-\frac{\tau_i}{2}}^{\frac{\tau_i}{2}} h^2 l_i^2 d\tau_i = h^2 l_i^2 \tau_i$, noise power (noise variance) is σ^2, SNR $\gamma = \frac{h^2 l_i^2 \tau_i}{\sigma^2}$) and average SNR $\bar{\gamma} = \frac{\tau_i l_i^2}{\sigma^2}$. PDF of instantaneous SNR for the Gaussian distribution function is given in Eq. (10) of [29]. Received data for the proposed modulation scheme is shown in Fig. 9, where T_1, T_2, T_3 and T_4 are the thresholds to differentiate the received data.

When the received data is other than the transmitted data, then the error occurs in the proposed system. Analytical BER expression for the hybrid multilevel pulse width modulation system is evaluated using the derivations of OOK given in [30]. The BER of the proposed modulation can be obtained using expression given in Eq. (8), shown at the bottom of the page, where

$$f_{i,j}(\gamma) = \frac{1}{\sqrt{2\pi\bar{\gamma}^2\sigma_{i,j}^2}} \exp\left(-\frac{(\gamma - \bar{\gamma}\mu_{i,j})^2}{2\bar{\gamma}^2\sigma_{i,j}^2}\right)$$

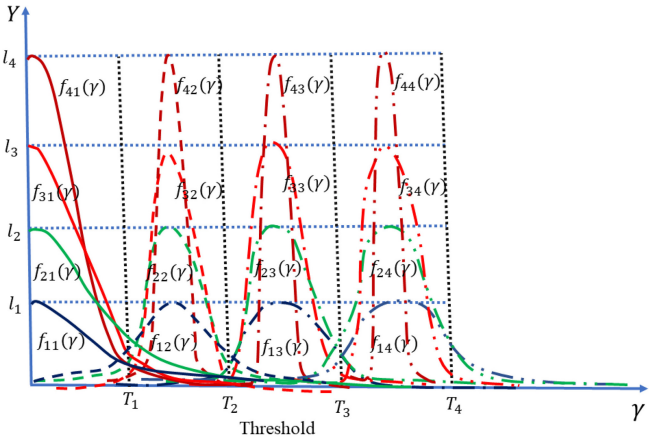

FIGURE 9. Received data for the proposed modulation.

here $\mu_{i,j}$ and $\sigma_{i,j}^2$ are mean and variance of $f_{i,j}(\gamma)$ and l_i is amplitude of received signal. There are two types of expressions in evaluating Eq. (8), which are given in ① and ②. After substituting ① and ② in Eq. (8) with the suitable integral limits, then the evaluated BER expression for the proposed modulation scheme using VLC link is given in Eq. (9), shown at the bottom of the page.

VI. EXPERIMENT RESULTS AND DISCUSSIONS

In this section, the results obtained from the experiment are presented. The experimental parameters are listed in Table 2. The experiment was conducted in an indoor environment

$$P_e = \frac{1}{16}\left(\int_{T_1}^{\infty} f_{11}(\gamma)d\gamma + \int_{0}^{T_1} f_{12}(\gamma)d\gamma + \int_{T_2}^{\infty} f_{12}(\gamma)d\gamma + \int_{0}^{T_2} f_{13}(\gamma)d\gamma + \int_{T_3}^{\infty} f_{13}(\gamma)d\gamma + \int_{0}^{T_3} f_{14}(\gamma)d\gamma + \cdots + \int_{0}^{T_2} f_{43}(\gamma)d\gamma + \int_{T_3}^{\infty} f_{43}(\gamma)d\gamma + \int_{0}^{T_3} f_{44}(\gamma)d\gamma\right) \tag{8}$$

$$① \Rightarrow \frac{1}{\sqrt{2\pi\bar{\gamma}^2\sigma_{ij}^2}} \int_0^T \exp\left(-\left(\frac{(x - \bar{\gamma}\mu_{ij})^2}{2\bar{\gamma}^2\sigma_{ij}^2}\right)\right)dx = \frac{1}{2}\left(erf\left(\frac{T - \bar{\gamma}\mu_{ij}}{\sqrt{2\bar{\gamma}^2\sigma_{ij}^2}}\right) + erf\left(\frac{\mu_{ij}}{\sqrt{2\sigma_{ij}^2}}\right)\right)$$

$$② \Rightarrow \frac{1}{\sqrt{2\pi\bar{\gamma}^2\sigma_{ij}^2}} \int_T^{\infty} \exp\left(-\left(\frac{(x - \bar{\gamma}\mu_{ij})^2}{2\bar{\gamma}^2\sigma_{ij}^2}\right)\right)dx = \frac{1}{2}\left(1 - erf\left(\frac{T - \bar{\gamma}\mu_{ij}}{\sqrt{2\bar{\gamma}^2\sigma_{ij}^2}}\right)\right)$$

$$P_e = \frac{1}{32}\sum_{i=1}^{4}\left(4 - erf\left(\frac{T_1 - \bar{\gamma}\mu_{i,1}}{\sqrt{2\bar{\gamma}^2\sigma_{i,1}^2}}\right) + erf\left(\frac{T_1 - \bar{\gamma}\mu_{i,2}}{\sqrt{2\bar{\gamma}^2\sigma_{i,2}^2}}\right) + erf\left(\frac{\mu_{i,2}}{\sqrt{2\sigma_{i,2}^2}}\right) - erf\left(\frac{T_2 - \bar{\gamma}\mu_{i,2}}{\sqrt{2\bar{\gamma}^2\sigma_{i,2}^2}}\right) + erf\left(\frac{T_2 - \bar{\gamma}\mu_{i,3}}{\sqrt{2\bar{\gamma}^2\sigma_{i,3}^2}}\right) + erf\left(\frac{\mu_{i,3}}{\sqrt{2\sigma_{i,3}^2}}\right) - erf\left(\frac{T_3 - \bar{\gamma}\mu_{i,3}}{\sqrt{2\bar{\gamma}^2\sigma_{i,3}^2}}\right) + erf\left(\frac{T_3 - \bar{\gamma}\mu_{i,4}}{\sqrt{2\bar{\gamma}^2\sigma_{i,4}^2}}\right) + erf\left(\frac{\mu_{i,4}}{\sqrt{2\sigma_{i,4}^2}}\right)\right) \tag{9}$$

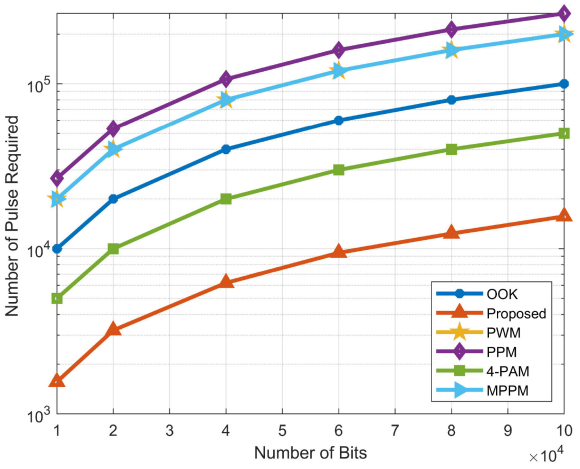

FIGURE 10. Comparison of different modulation techniques with the proposed technique in terms of data transmission efficiency; it is observed that the proposed modulation technique transmits the same amount of information using fewer optical pulses.

during nighttime, where the primary ambient source was a fluorescent light on the ceiling. The ambient-light intensity was 40-200 lux for the corridor and for a room environment 350-600 lux.

A. DATA TRANSMISSION EFFICIENCY AND TIME COMPLEXITY COMPARISON

Here, the data transmission efficiency achieved by the proposed technique is compared with other modulation techniques. Random data bits were generated as input values, and the number of pulses required to transmit the bits using different modulation techniques was calculated. We computed the number of optical pulses needed to transfer the same number of bits for different modulation techniques. A comparative analysis in terms of transmission efficiency of different modulation techniques is presented in Fig. 10. The x-axis represents the number of transmitted bits, and the y-axis represents the number of pulses required to transmit a specific the number of bits. In the PPM (represented by the top curve in Fig. 10 more pulses are required to transmit information because it wastes more bandwidth during a time interval. The next curve represents both the PWM and MPPM and exhibits better performance than PPM. The OOK exhibits better performance than the previous modulation techniques because only one pulse employed for each data bit. PAM can achieve better performance as compared to OOK. The proposed modulation technique outperforms all other techniques since it utilizes both the level and width of the signal. The curve of the proposed modulation technique shows it requires fewer pulses to transmit the same number of data bits.

The proposed modulation technique was compared with the existing modulation techniques in terms of time complexity. Figure 8 shows the test data frame length for different modulation techniques, here each division represents 1 ms. For comparison we have considered 0x2E(00101110) and 0x61(01100001) data sample. Figure 8(a) shows the data frame length when we apply PPM technique, which requires 5.760 ms to transmit the data. Next Fig. 8(b) shows MPPM which require 3.840 ms to transmit the data frame. For OOK modulation the transmission time reduced to 1.920 ms as depicted in Fig. 8(c). However, PWM has the similar time complexity as MPPM 3.840 as the requires same length in time to transmit 2 bits. Figure 8(d) represents the PWM time complexity. 4-PAM modulation can be more effective as compared to the other modulations as it requires only 0.960 ms to transmit the data frame as shown in Fig. 8(e). In case of the proposed modulation technique the required time for transmitting the frame is 0.450 ms. Which outperforms the other modulation techniques, because of the combined utilization of pulse width and height changes.

B. DATA BANDWIDTH

For the proposed modulation technique data-rate is depends on the width of the signal because it varies depending upon the bits generated by the transmitter. To find the data-rate we determine the cumulative number of pulses that are needed to transmit the data. We considered 30 μs as the unit of counting the width of a data segment. For any given segment the highest value is 4 and lowest value is 1. The data transmission rate can be calculate using the following equations:

$$D_{mpwm} = \frac{B}{n_t \times P} \tag{10}$$

$$n_t = \left\lceil \frac{\sum_{i=1}^{q} n_i}{4} \right\rceil \tag{11}$$

where $\lceil \cdot \rceil$ is ceiling operator. First we count the number of sub-segment q at 30 μs interval and divide by 4 to determine total single bit duration was utilized. Here we apply ceiling function to get the larger integer value. Next in Eq. (10), we calculate the data-rate, where D_{MPWM} is the data-rate for MPWM in bps, $B$is the number of transmitted bits, n_t is the total number of single bit duration, n is the number of pulses generated at each 4 bits combination, and P is pulse duration in seconds. The transmitted frame consists of 48 bits and using Eq. (11) we get 10 pulses. Each pulse duration is 120 s. By applying (10), a data-rate of 40,000 bps for the proposed modulation technique is obtained. For other modulation techniques we can calculate the data as:

$$D = \frac{B}{N \times P} \tag{12}$$

For data transmission with 120 μs pulse duration using OOK, a data transfer rate of 8,333 bps is obtained by using Eq. (12). This is less than 4 times than the proposed modulation. In the PWM and MPPM, the data-rate is the same (4,167 bps) because the number of pulses required is the same. In case of the 8-PPM, the data-rate low (approximately 3,125 bps) due to bandwidth wastage caused by the time-interval compensation. For 4-PAM the achieved data-rate is 16,666 bps which is double of OOK modulation.

TABLE 3. Data-rate comparison.

Single pulse time/ Bit duration (μs)	Modulation	Number of bits transmitted	Number of optical pulses	data-rate(bps)
120	OOK	100000	100000	8333
	8-PPM	100000	266667	3125
	MPPM	100000	200000	4167
	PWM	100000	200000	4167
	4-PAM	100000	50000	16666
	PAPM-PWM [19]	100000	133000	6250
	ML-MPPM[22]	100000	50000	16666
	PWM-PPM-DPAM[23]	100000	33334	25000
	MPWM	100000	22000	37499

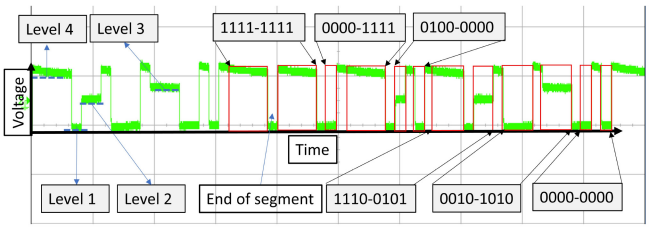

FIGURE 11. Data frame used in the experiment consisting of two header bytes (0xFF, 0x0F), the payload (0x40, 0xE5, 0x2A), and the end byte (0x00); this frame was captured by an oscilloscope at a 3 m distance.

A comparison of different modulations techniques in terms of data-rate is presented in Table 3. The proposed modulations data-rate varies with the input data stream.

C. BIT ERROR RATE INVESTIGATION

1) BER OF THE PROPOSED MODULATION

The proposed modulation technique was tested to determine the maximum achievable distance with the minimum bit error rate. A data frame, which was used to test the performance of the proposed modulation technique was created. This frame consists of three parts of 2 header bytes, the data payload, and the end byte. For the header, 0xFF (11111111) and 0x0F (00001111) were transmitted, indicating the start of the data frame. Subsequently, the data payload, was transmitted. In this case, we sent 0x40 (01000000), 0xE5 (11100101), and 0x2A (00101010) were transmitted. To mark the end of the frame, 0x00 (00000000) was added. An oscilloscope picture of this data frame is shown in Fig. 11. Each 4 bits are separated by an addition 30 μs pulse for demodulation purpose. Fig. 12 shows the received frame in different distance for the data-rate 40,000 bps. As the distance increases the received signal strength predeceases, thus the received frame voltage level decrease. Which causes inappropriate bit interpretation for different amplitude levels and introduces error in the communication. The experiment was conducted in the presence ambient light conditions 40-200 lux to observe the performance. As shown in the Fig. 11, data frame was transmitted and captured at the receiver end. We experimented with three different data-rates 40000, 20000, and 10000 bps. Different data-rate was achieved by changing the single pulse duration as 120 μs, 240 μs, and 480 μs. Figure 13 shows the

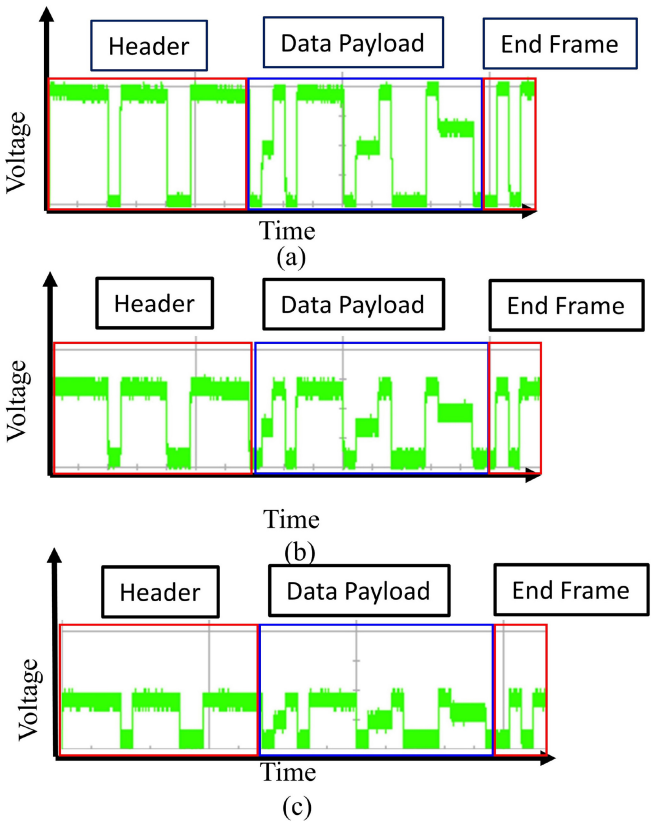

FIGURE 12. Data frame captured at different position during experiment for 40,000 bps; (a) the receiver is in 3m distance, (b) the receiver is in 3.25m distance, (c) the receiver is in 3.5m distance.

bit error rate (BER) performance of three different error rates. For the first data-rate 40,000 bps the distance is achieved 3 m and thereafter error rate increases dramatically. However, in the cased of 20,000 bps the communication distance is extended to 3.5 m as data-rate decreases. In case of 10,000 bps we can achieve more than 4 m distance. The error rate dramatically increases because of the threshold level can not detect all signals in defined range. In case of a room environment when the ambient light intensity is increased to 300-650 lux, the distance for MPWM is decreased. Figure 14 shows the error rate performance in indoor environment where the achievable distance in between 2.5-3.5 m.

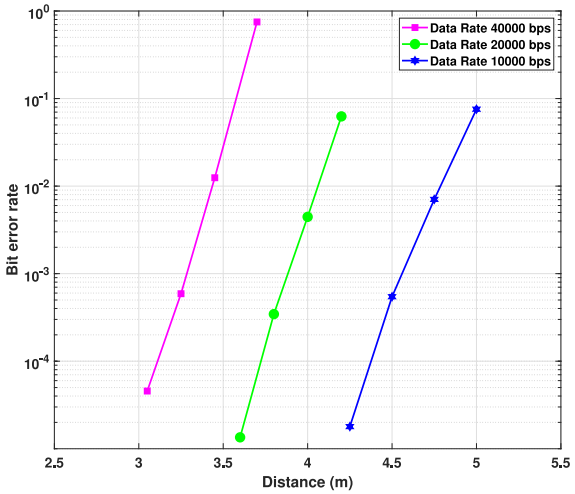

FIGURE 13. Experimental bit error rate performance of the proposed modulation with three different data-rates in a indoor corridor environment in the presence of 40-200 lux ambient light.

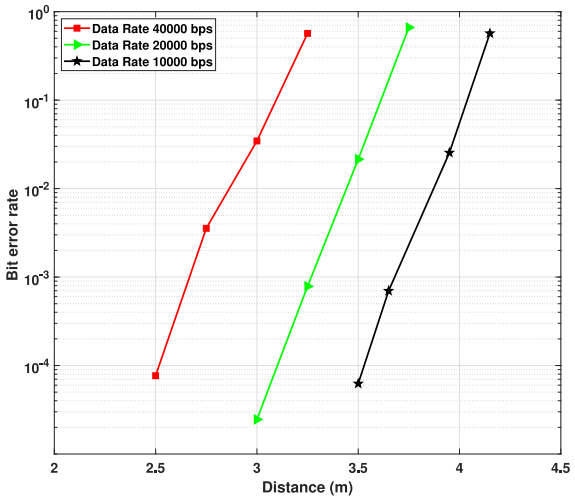

FIGURE 14. Experimental bit error rate performance of the proposed modulation with three different data-rates in a indoor room environment in the presence of 300-650 lux ambient light.

2) BIT ERROR RATE EXPERIMENTAL AND THEORETICAL OF THE PROPOSED MODULATION

Figure 15 shows the BER performance of the proposed hybrid pulse width modulation by means of experimental as well as theoretical analysis. The analytical BER results show that the close agreement with the experimental results. For the evaluating the analytical BER results, the mean, variance and threshold values are obtained from the experimental evaluation and substituted in Eq. (9). Table 5 shows the mean and variance of the each level of the proposed modulation technique. Thresholds and amplitude levels obtained from the experiments are: threshold levels $T = [1.303, 2.153, 2.903, 3.650]$ and amplitude levels $l = [0.750, 1.856, 2.45, 3.356]$. The variance due to the noise like thermal noise, shot noise and background noise are accumulated in the variances of the each level of hybrid modulation scheme. The theoretical BER result shows that

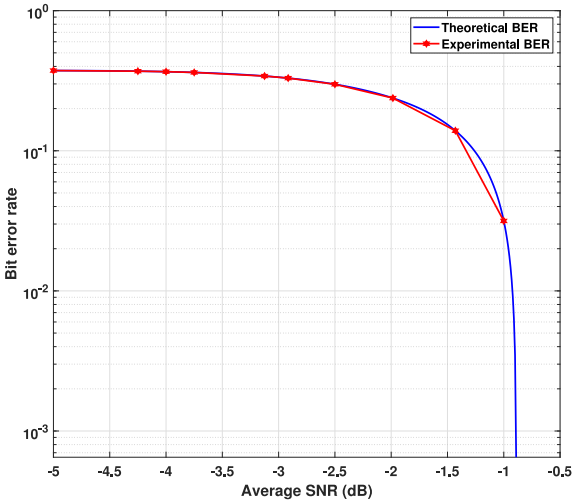

FIGURE 15. Bit error rate performance of the theoretical and experimental analysis of the proposed scheme with respect to average SNR.

TABLE 4. Simulation parameters.

Parameters	Values
Amplitude levels	
$l_1,\ l_2,\ l_3,\ l_4$	0.750, 1.856, 2.45, 3.356
Data rates	10, 20, 40 kbps
Duration	
$\tau_1,\ \tau_2,\ \tau_3,\ \tau_4$	30, 60, 90, 120 μs
Mean	Refer Table 5
Responsivity	0.45 A/W
Thresholds	
$T_1,\ T_2,\ T_3,\ T_4$	1.303, 2.153, 2.903, 3.650
Variance	Refer Table 5
Wavelength	620 nm

the average SNR of -1 dB needed to obtain 1×10^{-3} BER. The distance between the transmitter and receiver impacts the mean and variance of the received data, which results appropriate BER. Rytov variance (light scintillation due to atmospheric, related to mean and variance) is related to the distance between the transmitter-receiver is given as [31],

$$\sigma^2 = 1.23 C_n^2 k^{7/6} L^{11/6} \tag{13}$$

where C_n^2 is refractive index structure parameter and $C_n^2 = 10^{-17}\ m^{-2/3}$ for weak turbulence and $C_n^2 = 10^{-13}\ m^{-2/3}$ for strong turbulence regimes, $k = 2\pi/\lambda$ is wave-number and L is distance between the transmitter and receiver, wavelength $\lambda = 620$ nm. Mean and variance values obtained from the experiment are substituted in the BER derived expression. Simulation parameters of the proposed system are shown in Table 4. Fig. 16 shows the theoretical and experimental BER of the proposed system at 20000 bps data rate with respect to the distance between the transmitter and receiver. In intensity modulation direct detection system, the received voltage level is dependent on LED illumination. In the system, the four voltage levels can not be distinguished after 3.7 m specially 2-level and 3-level. A close correspondence between the

TABLE 5. Mean and variance values obtained from the experiment.

i,j	1,1	1,2	1,3	1,4	2,1	2,2	2,3	2,4
$\mu_{i,j}$	0.367	1.1172	1.8532	2.5031	0.367	1.1172	1.8532	2.5031
$\sigma^2_{i,j}$	0.0065	0.0364	0.0417	0.0454	0.0177	0.0991	0.1135	0.1237
i,j	**3,1**	**3,2**	**3,3**	**3,4**	**4,1**	**4,2**	**4,3**	**4,4**
$\mu_{i,j}$	0.367	1.1172	1.8532	2.5031	0.367	1.1172	1.8532	2.5031
$\sigma^2_{i,j}$	0.0318	0.1777	0.2037	0.2219	0.0409	0.2293	0.2628	0.2864

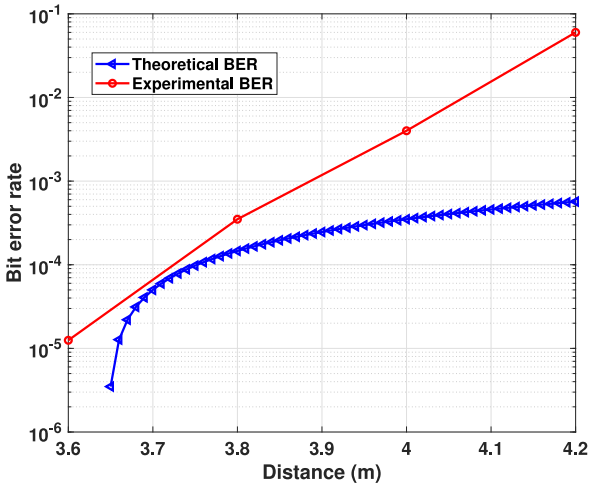

FIGURE 16. Theoretical and experimental BER with respect to distance between the transmitter and receiver.

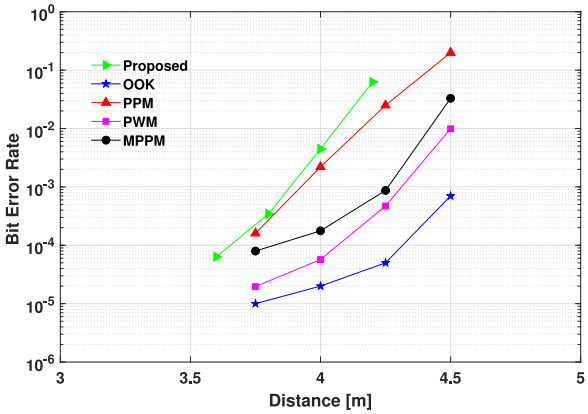

FIGURE 17. BER comparison of the proposed modulation technique with other modulations.

experimental and numerical BER results at 3.7 m distance between the transmitter and receiver.

3) BER COMPARISON WITH OTHER MODULATION TECHNIQUES

We have compared the BER performance of the proposed modulation technique with other modulation techniques. Figure 17 shows the result of the BER comparison of different modulation techniques. Here, all the modulation data are collected in the same experimental setup. It can be seen that the proposed modulation technique follows a similar trend to other modulation techniques, however, the error rate is a little high. This error rate can be mitigated by employing an efficient receiver which we will expand in our future studies.

D. DIMMING CONTROL

Dimming control is an important issue in indoor lighting, where communication must be preserved in different levels of dimming. In the proposed modulation technique we can change the dimming level by adding extra pulses beside the guard pulse. This will reduce the data rate but can be used to achieve a range of dimming range. The dimming level for a 4-bit segment is calculated by

$$dd = \tau_i * l_k \tag{14}$$

$$dg = l_n \tag{15}$$

$$dd\_t = \tau_i \tag{16}$$

$$dg\_t = l_n t \tag{17}$$

$$dim\_level = \frac{\sum_{k=1}^{n} dd_k + dg_k}{\sum_{j=1}^{n} dd\_t_j + l\_nt_j} \tag{18}$$

where, *dim_level* is the dimming level of a bit sequence, *dd* is the dimming level of four bit combination which includes $\tau_i \in \{1, 2, 3, 4\}$ is the width of the generated pulse, $l_k \in \{0.25, 0.5, 0.75, 1\}$ four different pulse levels, and d_g is the guard pulse level in which $l_n \in \{0.25, 1\}$ either low level or high level pulse. Again, dd_t is the dimming level when all pulses are in the highest level, which indicates full brightness and dg_t is a high guard pulse. The Eq. (18) represents the dimming level as the ratio of achieved brightness and total brightness. By applying Eq. (14) to (18) we can calculate the dimming level of the proposed modulation. The proposed frame as shown in Fig. 18 has a dimming level of 69%. Figure 18 shows a dimming control process for the proposed modulation. The dimming level can be increased if we add extra ten high pulses. The first five pulses are added after the header and the next five pulses are added before the end byte. The results show an increase in the dimming level which is now 75% as shown in Fig. 18(b). Similarly, to reduce the dimming level low pulses can be added to the same places to reduce the dimming level by 55% as shown in Fig. 18(c). However, the demodulation process needs to be adjusted by increasing at the same time to extract the correct bit patterns.

E. SPECTRAL EFFICIENCY

The spectral efficiency of the proposed system is a combined efficiency of PWM and PAM. The spectral efficiency for

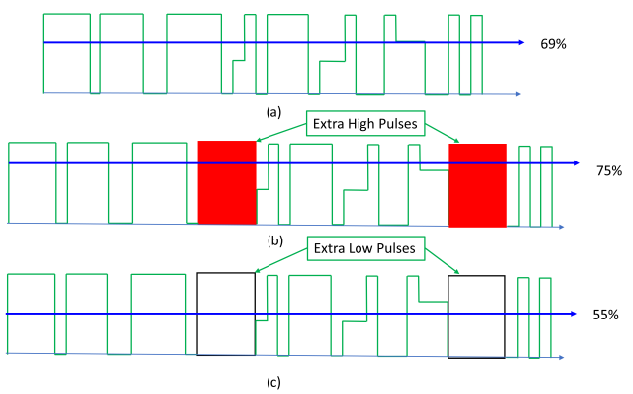

FIGURE 18. Dimming control mechanism for the proposed modulation technique; (a) shows the primary frame;(b) extra high pulses are added after the header and before end byte to increase the dimming level 75%; (c) extra low pulses are added after the header and before end byte to decrease the dimming level to 55%.

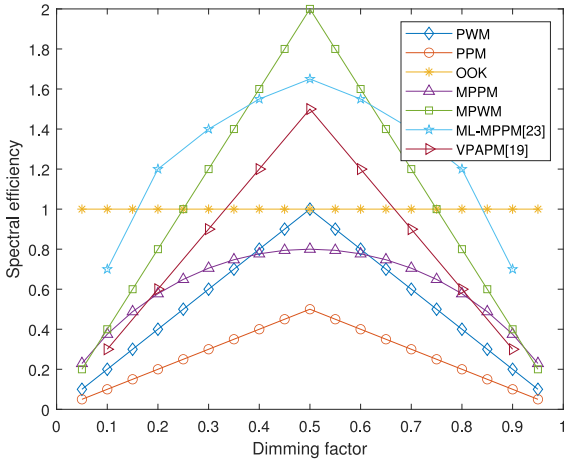

FIGURE 19. Spectral efficiency comparison with other modulation techniques.

PWM can be defined as:

$$pwm = \begin{cases} 2\gamma & 0 < \gamma \leq 0.5 \\ 2(1-\gamma) & 0.5 \leq \gamma < 1 \end{cases} \tag{19}$$

where γ is the dimming factor. In the case of PAM spectral efficiency can be defined as:

$$pam = \begin{cases} \gamma \log_2(M) & 0 < \gamma \leq 0.5 \\ (1-\gamma)\log_2(M) & 0.5 \leq \gamma < 1 \end{cases} \tag{20}$$

In our case the value of $M = 4$. Thus we can write:

$$pam = \begin{cases} 2\gamma & 0 < \gamma \leq 0.5 \\ 2(1-\gamma) & 0.5 \leq \gamma < 1 \end{cases} \tag{21}$$

So, the spectral efficiency of the proposed modulation is

$$mpwm = pwm * pam \tag{22}$$

which can be written as:

$$mpwm = 2pwm \tag{23}$$

Figure 19 shows the spectral efficiency performance comparison of the proposed MPWM with other modulation. It is clear from the Fig. 19 that the proposed modulation can achieve higher spectral efficiency.

F. COMPLEXITY ANALYSIS

Maximum likelihood estimation (MLE) employed for the identifying the amplitude levels signal, whereas for identifying the different pulse widths used low pass filter (integrator). Hence, with the 4-bit MLE, we achieve 8-bit demodulation using the proposed multi level hybrid pulse width modulation. The complexity of the system evaluated using the number of multiplication and additions involved in estimating the data [32]. The complexity involved for a $n-$bit MLE is $2^n \lfloor y - H\tilde{x} \rfloor$, here y is received data, H is $1 \times n$ channel fading coefficient, $\tilde{x}$ is one among 2^n combinations of $n \times 1$ estimated data. Hence, for a $8-$ bit modulation 2304 multiplications and 2304 additions, whereas the proposed modulation scheme evaluate same demodulation 80 multiplications and 80 additions. Further, the complexity of low pass filter depends upon the order of filter. In this paper, we have used a second order active low pass filter for the appropriate reproduction of various pulse widths.

VII. CONCLUSION

In this work, a hybrid MPWM technique to was proposed to improve the bandwidth efficiency for VLC. The proposed technique efficiently utilizes the available bandwidth by subdiving a single bit duration to impose more bits. As a result, it is capable of transmitting more data than other traditional modulation techniques. Therefore, it provides a good solution for IoT device communication in indoor short-range connectivity. The efficiency of the proposed modulation technique was experimentally demonstrated by achieving a communication distance of 3 m in an indoor environment. Its performance was evaluated by measuring the communication BER. In addition, we have evaluated the theoretical BER analysis of the proposed system, and compared the BER performance obtained using the proposed experimental setup. The modulation's data-rate can be adjusted by changing the single bit duration. The proposed modulation is suitable for short-distance communication, and an indoor lightning environment is preferred. Another advantage of the proposed system is a simple design circuit with 9 LEDs and 1 photodiode as the transmitter and receiver. Which can be implemented with low-cost and low-complexity circuit design. There are some scopes available for further investigation. To increase the communication distance an efficient receiver design can be studied. How much speed can be achieved which can be achievable can also be investigated with high speed communication devices. Efficient dimming control strategy can be investigated to counter the data rate degradation. In our future study, we want to enhance the link range of the VLC link by incorporating the forward error control codes and multiple input to multiple output schemes with the improved reliable data transmission.

TABLE 6. Threshold values for 40-200 lux condition.

Distance	level 1 (V)	level 2 (V)	level 3 (V)	level 4 (V)
3 m	0 - 1.5	1.6 - 2.0	2.0 - 2.5	2.8 - 3.5
3.25 m	0 - 1.3	1.5 - 1.8	1.8 - 2.2	2.2 - 2.6
3.50 m	0 - 0.5	0.5 - 0.8	0.8 - 1.2	1.2 - 1.6

TABLE 7. Threshold values for 300-650 lux condition.

Distance	level 1 (V)	level 2 (V)	level 3 (V)	level 4 (V)
2.5 m	0 - 1.1	1.1 - 1.5	1.5 - 1.8	1.8 - 2.5
2.75 m	0 - 0.7	0.7 - 1.0	1.0 - 1.5	1.5 - 1.9
3.00 m	0 - 0.35	0.35 - 0.6	0.6 - 1.0	1.0 - 1.4

APPENDIX

The threshold range of voltage at different distances is given in the Tables 6 and 7.

REFERENCES

[1] L. Feng, R. Q. Hu, J. Wang, P. Xu, and Y. Qian, "Applying VLC in 5G networks: Architectures and key technologies," *IEEE Netw.*, vol. 30, no. 6, pp. 77–83, Nov./Dec. 2016.

[2] L. Teixeira, F. Loose, J. P. Brum, C. H. Barriquello, V. A. Reguera, and M. A. D. Costa, "On the LED illumination and communication design space for visible light communication," *IEEE Trans. Ind. Appl.*, vol. 55, no. 3, pp. 3264–3273, May/Jun. 2019.

[3] M. A. S. Sejan and W.-Y. Chung, "Lightweight multi-hop VLC using compression and data-dependent multiple pulse modulation," *Opt. Exp.*, vol. 28, no. 13, pp. 19531–19549, 2020.

[4] L. U. Khan, "Visible light communication: Applications, architecture, standardization and research challenges," *Digit. Commun. Netw.*, vol. 3, no. 2, pp. 78–88, 2017.

[5] M. A. S. Sejan and W.-Y. Chung, "Indoor fine particulate matter monitoring in a large area using bidirectional multihop VLC," *IEEE Internet Things J.*, vol. 8, no. 9, pp. 7214–7228, May 2021.

[6] D. Singh, C. Basu, M. Meinhardt-Wollweber, and B. Roth, "LEDs for energy efficient greenhouse lighting," *Renew. Sustain. Energy Rev.*, vol. 49, pp. 139–147, Sep. 2015.

[7] M. S. Islim and H. Haas, "Modulation techniques for Li-Fi," *ZTE Commun.*, vol. 14, no. 2, pp. 29–40, 2019.

[8] S. H. Lee, S.-Y. Jung, and J. K. Kwon, "Modulation and coding for dimmable visible light communication," *IEEE Commun. Mag.*, vol. 53, no. 2, pp. 136–143, Feb. 2015.

[9] S. Rajagopal, R. D. Roberts, and S.-K. Lim, "IEEE 802.15.7 visible light communication: Modulation schemes and dimming support," *IEEE Commun. Mag.*, vol. 50, no. 3, pp. 72–82, Mar. 2012.

[10] D. Karunatilaka, F. Zafar, V. Kalavally, and R. Parthiban, "LED based indoor visible light communications: State of the art," *IEEE Commun. Surveys Tuts.*, vol. 17, no. 3, pp. 1649–1678, 3rd Quart., 2015.

[11] V. P. Rachim and W.-Y. Chung, "Multilevel intensity-modulation for rolling shutter-based optical camera communication," *IEEE Photon. Technol. Lett.*, vol. 30, no. 10, pp. 903–906, May 15, 2018.

[12] D. Kim, J. K. Park, and J. T. Kim, "High-efficient and low-cost biased multilevel modulation technique for IM/DD-based VLP systems," *IEEE Access*, vol. 8, pp. 218954–218965, 2020.

[13] M. K. Hasan, N. T. Le, M. Shahjalal, M. Z. Chowdhury, and Y. M. Jang, "Simultaneous data transmission using multilevel LED in hybrid occ/lifi system: Concept and demonstration," *IEEE Commun. Lett.*, vol. 23, no. 12, pp. 2296–2300, Dec. 2019.

[14] S.-J. Kim, J.-W. Lee, D.-H. Kwon, and S.-K. Han, "Gamma function based signal compensation for transmission distance tolerant multilevel modulation in optical camera communication," *IEEE Photon. J.*, vol. 10, no. 5, pp. 1–7, May 2018.

[15] M. Le-Tran and S. Kim, "Enhanced multi-level multi-pulse modulation for MIMO visible light communication," *IEEE Access*, vol. 8, pp. 210116–210126, 2020.

[16] J.-H. Choi, E.-B. Cho, T.-G. Kang, and C. G. Lee, "Pulse width modulation based signal format for visible light communications," in *OECC Tech. Dig.*, 2010, pp. 276–277.

[17] A. Pradana, N. Ahmadi, and T. Adionos, "Design and implementation of visible light communication system using pulse width modulation," in *Proc. IEEE Int. Conf. Elect. Eng. Inf. (ICEEI)*, 2015, pp. 25–30.

[18] J.-W. Lee, S.-H. Yang, and S.-K. Han, "Optical pulse width modulated multilevel transmission in CIS-based VLC," *IEEE Photon. Technol. Lett.*, vol. 29, no. 15, pp. 1257–1260, Aug. 2017.

[19] L. Yi and S. G. Lee, "Performance improvement of dimmable VLC system with variable pulse amplitude and position modulation control scheme," in *Proc. IEEE Int. Conf. Wireless Commun. Sensor Netw.*, 2014, pp. 81–85.

[20] G. Ntogari, T. Kamalakis, J. Walewski, and T. Sphicopoulos, "Combining illumination dimming based on pulse-width modulation with visible-light communications based on discrete multitone," *J. Opt. Commun. Netw.*, vol. 3, no. 1, pp. 56–65, 2011.

[21] H.-J. Jang, J.-H. Choi, Z. Ghassemlooy, and C. G. Lee, "PWM-based PPM format for dimming control in visible light communication system," in *Proc. 8th Int. Symp. Commun. Syst. Netw. Digit. Signal Process. (CSNDSP)*, 2012, pp. 1–5.

[22] A. B. Siddique and M. Tahir, "Bandwidth efficient multi-level MPPM encoding decoding algorithms for joint brightness-rate control in VLC systems," in *Proc. IEEE Global Commun. Conf.*, 2014, pp. 2143–2147.

[23] Y. Xu et al., "Hybrid modulation scheme for visible light communication using CMOS camera," *Opt. Commun.*, vol. 440, pp. 89–94, Jun. 2019.

[24] J.-J. Bao, C.-L. Hsu, and J.-F. Tu, "An efficient data transmission with GSM-MPAPM modulation for an indoor VLC system," *Symmetry*, vol. 11, no. 10, p. 1232, 2019.

[25] A. R. Ndjiongue and H. C. Ferreira, "Hybrid trellis coded modulation (HTCM) for visible light communications," *IET Commun.*, vol. 13, no. 1, pp. 85–92, 2019.

[26] H. S. Khallaf, A. E. Morra, A. E. Elfiqi, H. M. Shalaby, and S. Hranilovic, "Hybrid two-level MPPM–MDPSK modulation for high-speed optical communication networks," *Appl. Opt.*, vol. 58, no. 36, pp. 9757–9767, 2019.

[27] P. K. Sahoo, Y. K. Prajapati, and R. Tripathi, "PPM-and GMSK-based hybrid modulation technique for optical wireless communication cellular backhaul channel," *IET Commun.*, vol. 12, no. 17, pp. 2158–2163, 2018.

[28] L. Mao, C. Li, H. Li, X. Chen, X. Mao, and H. Chen, "A mixed-interval multi-pulse position modulation scheme for real-time visible light communication system," *Opt. Commun.*, vol. 402, pp. 330–335, Nov. 2017.

[29] R. P. Naik, P. Krishnan, and G. G. Simha, "Reconfigurable intelligent surface-assisted free-space optical communication system under the influence of signal blockage for smart-city applications," *Appl. Opt.*, vol. 61, no. 20, pp. 5957–5964, 2022.

[30] R. P. Naik, U. S. Acharya, S. Lal, and P. Krishnan, "Performance investigation of underwater wireless optical system for image transmission through the oceanic turbulent optical medium," *Opt. Quant. Electron.*, vol. 54, no. 4, pp. 1–16, 2022.

[31] R. Pernice et al., "Indoor free space optics link under the weak turbulence regime: Measurements and model validation," *IET Commun.*, vol. 9, no. 1, pp. 62–70, 2015.

[32] S. G. Shashikant, G. Simha, and U. S. Acharya, "Generalized designs for precoded receive spatial modulation derived from non-orthogonal space time block codes," *Telecommun. Syst.*, vol. 79, no. 3, pp. 405–416, 2022.

MOHAMMAD ABRAR SHAKIL SEJAN (Member, IEEE) received the B.S. and M.S. degrees in computer science and engineering from Islamic University, Kushtia, Bangladesh, in 2014 and 2016 respectively, and the Ph.D. degree from the Department of Electronic Engineering, Pukyong National University, Busan, South Korea, in 2022.

His research interests includes visible light communication, optical communication, wireless sensor networks, protocol design for communication, modulation techniques in VLC, and multi-hop communication and IoT applications. He has published several papers in reputed journals and also servers as a reviewer in different journals and conferences.

RAMAVATH PRASAD NAIK received the M.Tech. degree from the Department of Electronics and Communication Engineering, Motilal Nehru National Institute of Technology Allahabad, Allahabad, India, in 2015, and the Ph.D. degree from the National Institute of Technology Karnataka, Mangalore, India, in 2021.

He is currently a Postdoctoral Researcher with the Department of Research, Institute of Artificial Intelligence Convergence, Pukyong National University, Busan, South Korea. His research interests include free-space and underwater optical wireless communication, theory and application of error control codes, and co-operative communication applications.

BOON GIIN LEE (Senior Member, IEEE) received the B.I.T. degree in information technology from Multimedia University, Melaka, Malaysia, in 2007, the M.S. degree in electronic engineering from Dongseo University, Busan, South Korea, and the Ph.D. degree in electronic engineering from Pukyong National University, Busan.

From 2013 to 2014, he worked as a Software Engineer with Changsung Ace Company, Seoul, South Korea. After this, from 2014 to 2019, he was employed as Assistant Professor with Department of Electronic Engineering, Keimyung University, South Korea. Since 2019, he has been with the School of Computer Science, The University of Nottingham Ningbo China, where he was an Assistant Professor and became an Associate Professor since 2022. He is the Head of Smart Firefighting Operations System Laboratory with CBI and Human-Computer Interaction Research Laboratory with UNNC. His research interests lie in the area of human-computer interaction, deep learning, computer vision, and smart wearable sensing. He was a recipient of the IEEE SENSORS JOURNAL Best Paper Award in 2019.

WAN-YOUNG CHUNG (Senior Member, IEEE) received the B.S. and M.S. degrees in electronic engineering from Kyungpook National University, Daegu, South Korea, in 1987 and 1989, respectively, and the Ph.D. degree in sensor engineering from Kyushu University, Fukuoka, Japan, in 1998.

He was an Assistant Professor with Semyung University, from 1993 to 1999, and an Associate Professor with Dongseo University from 1999 to 2008. He has been a Full Professor with the Department of Electronic Engineering, Pukyong National University, South Korea, since September 2008. His research interests include artificial intelligence, ubiquitous healthcare, wireless sensor network applications, and gas sensors. He serves as an Associate Editor for IEEE SENSORS JOURNAL.